*American Mineralogist, Volume 61, pages 303–310, 1976*

# The thermal expansion of diopside to 800°C and a refinement of the crystal structure at 700°C

LARRY W. FINGER AND YOSHIKAZU OHASHI

*Geophysical Laboratory, Carnegie Institution of Washington*
*Washington, D. C. 20008*

**Abstract**

The crystal structure of diopside from Twin Lakes, California, has been refined to a weighted residual of 4.2 percent from intensity data collected at 700°C. The results of this study are virtually identical with those of Cameron, Sueno, Prewitt, and Papike (1973) at the same temperature. In addition, strain ellipsoids describing the thermal expansion for this material have been calculated from the unit-cell parameters determined at nine different temperatures. The values given by Cameron *et al.* (1973) and Deganello (1973) for other diopsides have been used in similar calculations. These results clearly show that the minimum expansion direction is along the shortest Ca–O bond distance rather than parallel to the tetrahedral chain. The direction of maximum expansion is parallel to the *b* axis.

## Introduction

There are many recent studies of crystal structures at elevated temperatures; however, there has been very little comparison of the results obtained in the various laboratories using different data collection techniques and crystal heater designs. This study was undertaken to provide such a comparison of the resulting structure refinement, to check the operating procedures of the Geophysical Laboratory computer-controlled, high-temperature diffractometer system (Finger, Hadidiacos, and Ohashi, 1973; Finger, 1973), and to evaluate the strain tensor method (Ohashi and Burnham, 1973; Ohashi and Finger, 1973) in presenting thermal expansion data.

Diopside was chosen as the subject of this study because the results of several studies are available for comparison. The structure at room temperature was solved by Warren and Bragg (1928) and was subsequently refined by Clark, Appleman, and Papike (1968, 1969). The structure has been refined at several elevated temperatures by Cameron *et al.* (1973, hereafter referred to as CSPP). This study attempts to verify their results at 700°C. In addition to the high-temperature unit-cell data presented by CSPP, Deganello (1973) has measured the unit cell of diopside at elevated structures using a powder diffraction technique, and Nolan and Edgar (1963) reported the unit-cell parameters for a synthetic diopside; consequently there are abundant results with which to evaluate the strain tensor method.

## Data collection

### *Unit cell*

An analyzed sample of diopside from Twin Lakes, California (collected and described by Chesterman, 1942), was kindly provided by Dr. H. S. Yoder, Jr. The results of gravimetric and spectrometric analyses by E. Martinec and N. H. Suhr (Yoder, personal communication) and an electron microprobe analysis (R. H. McCallister, personal communication) are listed in Table 1. A crystal with the approximate dimensions 0.06 × 0.11 × 0.30 mm was mounted in an arbitrary orientation on a fused silica capillary using finely ground zirconia and Zircoa Bond 6 as a high-temperature adhesive. After the cement was cured at 200°C for several hours, the crystal was mounted on the four-circle diffractometer, and the orientation and approximate unit cell of the crystal were determined. After a preliminary refinement of the unit-cell parameters, twelve relatively intense reflections with $2\theta > 45°$ for Mo$K\alpha_1$ radiation were selected and used in the final refinement. The optimum diffractometer angles for each of these reflections were automatically determined using the centering procedure of Busing (1970), and the refined orientation matrix and unit-cell parameters were determined using the method of Gabe, Alexander, and Goodman (1970), which is similar to that of Tichy (1970).

The temperature of the furnace used in this study

TABLE 1. Chemical analysis and mineral formula for diopside from Twin Lakes, California

| Oxide | Wt. %* | Wt. %** | Cations/6 Oxygens |
|---|---|---|---|
| $SiO_2$ | 55.36 | 55.7 | 1.99*** |
| $Al_2O_3$ | 0.00 | 0.07 | 0.00 |
| $TiO_2$† | 0.01 | n.d.†† | |
| $V_2O_5$† | 0.00 | n.d. | |
| $Cr_2O_3$ | 0.00 | 0.00 | |
| FeO††† | 0.09 | 0.09 | 0.00 |
| NiO† | 0.00 | n.d. | |
| MnO | 0.005 | 0.00 | |
| MgO | 18.77 | 18.8 | 1.00 |
| CaO | 25.70 | 26.0 | 1.00 |
| $Li_2O$ | 0.00 | n.d. | |
| $Na_2O$ | 0.02 | 0.02 | |
| $K_2O$ | 0.00 | n.d. | |
| $H_2O^+$ | 0.00 | n.d. | |
| $H_2O^-$ | 0.00 | n.d. | |
| $P_2O_5$ | 0.06 | 0.00 | |
| BeO† | <0.005 | n.d. | |
| CuO† | <0.01 | n.d. | |
| $ZrO_2$ | <0.03 | n.d. | |
| | 100.01 | 100.8 | 4.00 |

*Analyst: E. Martinec, Pennsylvania State University.
**Electron microprobe analysis by R. H. McCallister, Geophysical Laboratory.
***Chemical formula calculated from the electron microprobe analysis.
†Spectrochemical determination by N. H. Suhr, Pennsylvania State University.
††n.d., not determined.
†††Total iron as FeO.

can be changed under program control. This facility was used to measure the unit-cell parameters of the crystal at 100° intervals from 100° to 800°C. The crystal was heated in air without apparent damage. The refined unit-cell parameters are listed in Table 2, and the results are discussed below.

### *Intensity collection*

After the measurement of the unit-cell data described above, the crystal was again heated in air to 700°C, and the integrated intensities for all reflections with $\sin\theta/\lambda > 0.705$ were measured using Nb-filtered Mo radiation. A $\theta$-$2\theta$ scan technique was employed, the scan range being calculated from the equation $\Delta 2\theta = 2.0 + 0.7 \tan\theta$ (degrees). The background counting time and scan rate were adjusted to achieve a constant value for the ratio of the intensity to its standard deviation. In this method, an initial estimate of the intensity is made from short counts at the peak and background positions. The optimum peak and background counting times may then be calculated (Finger *et al.*, 1973) to minimize the time of data collection without reducing the precision of the results. In the intensity collection, a pair standard reflections was remeasured every 2 hours. There was no significant drift over the 54-hour period required for data collection.

The integrated intensities were corrected for the Lorentz-polarization and absorption ($\mu_l$ = 18.8 $cm^{-1}$) effects using a program modified from Burnham (1966). This program also calculates the geometric factor used in the secondary extinction correction of Zachariasen (1968). The mass absorption coefficients used in the calculation of $\mu_l$ were taken from Cromer and Liberman (1970).

### Crystal structure refinement

The observed structure factors, with weights calculated from counting statistics, and the refined parameters of CSPP were used as input to the least-squares program RFINE (Finger and Prince, 1975). Neutral scattering factors of Cromer and Mann (1968) and the anomalous scattering coefficients of Cromer and Liberman (1970) were used with an assumed composition of $CaMgSi_2O_6$. The composition of the material, as determined by the electron microprobe, deviates by less than 1 mole percent from the ideal

TABLE 2. Results of unit-cell determination at various temperatures for diopside from Twin Lakes, California

| T, °C | a, Å | b, Å | c, Å | β, degrees | V, Å$^3$ |
|---|---|---|---|---|---|
| 24 | 9.753(4)* | 8.922(3) | 5.249(2) | 105.95(3) | 439.1(2) |
| 100† | 9.756(4) | 8.936(3) | 5.252(1) | 105.99(2) | 440.2(3) |
| 200 | 9.758(7) | 8.949(7) | 5.253(3) | 105.88(5) | 441.3(5) |
| 300 | 9.770(7) | 8.954(7) | 5.258(3) | 105.94(5) | 442.3(5) |
| 400 | 9.774(5) | 8.979(4) | 5.264(1) | 105.89(3) | 444.3(3) |
| 500 | 9.784(3) | 8.997(2) | 5.267(1) | 105.94(2) | 445.8(2) |
| 600 | 9.795(3) | 9.015(2) | 5.272(1) | 105.96(2) | 447.5(2) |
| 700 | 9.804(5) | 9.030(3) | 5.275(2) | 105.98(3) | 449.0(3) |
| 800 | 9.810(6) | 9.054(6) | 5.277(3) | 106.02(5) | 450.6(5) |

*The number in parentheses represents the estimated standard deviation of the final digit presented. This notation will be used throughout this paper.
†The errors in the temperatures are not well known but are approximately ±20°C for some temperatures.

formula. The structure was initially converged with isotropic temperature factors, which were converted to anisotropic for the final refinement. The atomic positions, anisotropic vibration tensor coefficients, a scale factor, and the isotropic extinction factor (Zachariasen, 1968) were varied. The results of this refinement are listed in Table 3, and the observed and calculated structure factors are available.[1] Table 4 gives the final values for the atomic positions, the anisotropic temperature factor coefficients, and the equivalent isotropic temperature factors (Hamilton, 1959).

TABLE 3. Intensity data collection information for diopside from Twin Lakes, California, at 700°C

| | |
|---|---|
| Space group | C2/c |
| Crystal size | 0.06 x 0.11 x 0.30 mm |
| No. of reflections | 725 |
| No. of observed reflections* | 558 |
| Wtd. r, all data** | 4.9% |
| R, all data† | 7.3% |
| Wtd. r, observed reflections | 4.2% |
| R, observed reflections | 5.2% |
| Extinction coefficient | $1.3(1) \times 10^{-5}$ cm |

*The reflections with an intensity less than twice the standard deviation (162) and those with $\Delta F > 6(5)$ are not included with the observed reflections.

**Wtd. $r = [\Sigma w(|F_o| - |F_c|)^2 / \Sigma w F_o^2]^{1/2}$

†$R = \Sigma||F_o| - |F_c||/\Sigma|F_o|$

## Discussion of refined structure

### *Thermal ellipsoids*

The functional dependence of the structure factors on the thermal parameters is similar to that of many other factors, such as absorption and extinction. In addition any crystal imperfections that tend to delocalize the atoms will affect the temperature factors. For these reasons, the comparison of thermal ellipsoids from one structure refinement to another is not generally attempted. If such a comparison is attempted, the agreement of the ellipsoid sizes may be checked by inspecting the *rms* amplitude; the orientations, however, are not so easily compared. One means of making this comparison is to compute the angle required to rotate one ellipsoid into the other. If $\mathbf{V}_1$ is a $3 \times 3$ matrix with columns equal to the direction cosines of the principal axes relative to an arbitrary orthogonal coordinate system for one thermal ellipsoid, and $\mathbf{V}_2$ is a similar vector for a second ellipsoid, the rotation operation is described by a matrix $\mathbf{A}$ satisfying the equation

$$\mathbf{V}_1 = \mathbf{A}\mathbf{V}_2$$

or

$$\mathbf{A} = \mathbf{V}_1\mathbf{V}_2^{-1} \tag{1}$$

The angle of rotation ($\delta$) and direction cosines of the axis of rotation ($c_1$, $c_2$, $c_3$) are given in standard mathematical reference texts (for example, Korn and Korn, 1961, p. 412) as follows:

$$\begin{aligned} \cos\delta &= \tfrac{1}{2}(a_{11} + a_{22} + a_{33} - 1) \\ c_1 &= \tfrac{1}{2}(a_{32} - a_{23})/\sin\delta \\ c_2 &= \tfrac{1}{2}(a_{13} - a_{31})/\sin\delta \\ c_3 &= \tfrac{1}{2}(a_{21} - a_{12})/\sin\delta \end{aligned} \tag{2}$$

with $a_{ij}$ equal to the $ij$th element of $\mathbf{A}$. A BASIC

[1] To receive a copy of this material, order document AM-76-014 from the Business Office, Mineralogical Society of America, 1909 K Street, N.W., Washington, D. C. 20006. Please remit in advance $1.00 for the microfiche.

TABLE 4. Final positions and anistropic temperature factors* for diopside from Twin Lakes, California, at 700°C

| Atom | x | y | z | $B_{eq}$** | $\beta_{11}$ | $\beta_{22}$ | $\beta_{33}$ | $\beta_{12}$ | $\beta_{13}$ | $\beta_{23}$ |
|---|---|---|---|---|---|---|---|---|---|---|
| M1† | 0 | 0.9067(3) | 1/4 | 1.50(4) | 49(3) | 40(3) | 147(10) | 0 | 28(4) | 0 |
| M2 | 0 | 0.3003(2) | 1/4 | 2.26(4) | 82(2) | 43(2) | 208(8) | 0 | 7(4) | 0 |
| Si | 0.2864(1) | 0.0923(2) | 0.2299(3) | 1.15(3) | 32(1) | 30(2) | 137(6) | -3(2) | 27(2) | -4(3) |
| O1 | 0.1167(3) | 0.0872(4) | 0.1417(7) | 1.53(6) | 39(4) | 51(5) | 155(14) | -11(4) | 25(6) | -3(7) |
| O2 | 0.3617(4) | 0.2460(4) | 0.3166(7) | 2.02(7) | 70(5) | 41(4) | 223(18) | -24(4) | 41(7) | -30(7) |
| O3 | 0.3493(3) | 0.0155(4) | 0.9978(6) | 1.65(6) | 42(4) | 58(5) | 163(15) | 3(4) | 31(6) | -28(7) |

*The anisotropic temperature factors $\beta$, here given $\times 10^5$, are of the form $\exp\{-\sum_j \sum_k h_j h_k \beta_{jk}\}$.

**The equivalent isotropic temperature factor, $B_{eq}$, is computed according to the formulations of Hamilton (1959).

†Atom nomenclature is that proposed by Burnham, Clark, Papike, and Prewitt (1967).

program (available upon request) for calculation of these parameters has been written.

The principal components of the thermal ellipsoids of this study from program BONDAN (Finger and Prince, 1975) are presented in Table 5 with the *rms* amplitudes of the results of CSPP at 700°C and the angle $\delta$ required to rotate one ellipsoid into the other. When the *rms* amplitudes of the two studies are compared, only the largest values for $M1$ and O2 and the intermediate one for $M2$ differ by as much as two standard deviations. The agreement is remarkable, particularly when the differences in starting material, data collection, and corrections employed are considered. The uncertainties in the rotation angles have not been calculated but are probably of the order of 20 to 30°; thus the ellipsoid for $M1$ from this study clearly differs significantly from that of CSPP. The results of this study indicate a triaxial ellipsoid with the shortest axis parallel to $b$, whereas CSPP obtained an ellipsoid that was essentially an oblate spheroid with the unique axis having angles of 42°, 90°, and 64° with $a$, $b$, and $c$, respectively.

### *Bond functions*

The interatomic distances and angles for this study from program BONDAN are presented in Table 6. Figure 1 may be used to aid in the interpretation of this table. As discussed by Busing and Levy (1964), the mean separation of two atoms must be corrected for the effects of thermal vibration. Unfortunately, a model for the interactions between the two atoms must be assumed before this correction can be made. The interatomic forces in a pyroxene are rather complicated for the construction of such a model; however, Busing and Levy have provided the formulations for four interaction schemes. Two of

TABLE 5. Principal axes of thermal ellipsoids for diopside at 700°C

| Atom | rms amplitude, Å | | Angle (°) with | | | Rotation Angle, $\delta$* (°) |
|---|---|---|---|---|---|---|
| | This Study | Cameron et al (1973) | a | b | c | |
| M1 | 0.129(5) | 0.128(2) | 90 | 0 | 90 | 89 |
| | 0.135(5) | 0.135(2) | 63(16) | 90 | 169(16) | |
| | 0.149(4) | 0.137(2) | 153(16) | 90 | 101(16) | |
| M2 | 0.133(3) | 0.139(1) | 90 | 0 | 90 | 4 |
| | 0.156(3) | 0.143(1) | 110(3) | 90 | 144(3) | |
| | 0.208(3) | 0.203(1) | 160(3) | 90 | 54(3) | |
| Si | 0.109(3) | 0.104(1) | 57(19) | 33(20) | 100(13) | 38 |
| | 0.115(3) | 0.121(1) | 39(19) | 121(21) | 125(7) | |
| | 0.136(3) | 0.131(1) | 109(5) | 79(6) | 144(6) | |
| O1 | 0.118(8) | 0.112(3) | 33(9) | 57(9) | 104(14) | 41 |
| | 0.141(7) | 0.149(3) | 97(18) | 79(19) | 14(14) | |
| | 0.155(7) | 0.152(3) | 58(9) | 144(10) | 86(22) | |
| O2 | 0.105(9) | 0.119(4) | 68(4) | 28(3) | 78(5) | 36 |
| | 0.166(7) | 0.165(3) | 53(9) | 89(7) | 159(9) | |
| | 0.195(6) | 0.182(3) | 135(8) | 62(3) | 108(10) | |
| O3 | 0.115(8) | 0.121(3) | 129(11) | 58(6) | 44(7) | 10 |
| | 0.142(6) | 0.139(3) | 140(12) | 108(11) | 110(11) | |
| | 0.171(7) | 0.176(3) | 98(9) | 142(7) | 52(6) | |

*Angle required to rotate the ellipsoid of this study into the ellipsoid of Cameron et al (1973). See text for the details of the calculation.

TABLE 6. Selected interatomic distances and angles for diopside at 700°C

| Atoms | Interatomic Distances, Å | | | Oxygen-Cation-Oxygen Angle, Degrees |
|---|---|---|---|---|
| | Uncorrected | Corrected* for Parallel, Highly Correlated Motion | Corrected for Noncorrelated Motion | |
| Si tetrahedron | | | | |
| Si-O1C1† | 1.600(3) | 1.600 | 1.622 | |
| Si-O2C1 | 1.579(4) | 1.581 | 1.610 | |
| Si-O3C1 | 1.666(3) | 1.667 | 1.690 | |
| Si-O3C2 | 1.687(4) | 1.687 | 1.708 | |
| Mean | 1.633 | 1.634 | 1.658 | |
| O1C1-O2C1 | 2.731(5) | 2.731 | 2.749 | 118.4(2) |
| O1C1-O3C1 | 2.673(4) | 2.673 | 2.690 | 109.9(2) |
| O1C1-O3C2 | 2.689(5) | 2.689 | 2.703 | 109.8(2) |
| O2C1-O3C1 | 2.657(5) | 2.658 | 2.677 | 109.9(2) |
| O2C1-O3C2 | 2.563(5) | 2.563 | 2.583 | 103.4(2) |
| O3C1-O3C2 | 2.652(1) | 2.652 | 2.668 | 104.6(1) |
| Mean | 2.661 | 2.661 | 2.678 | |
| | | | Angle O3-O3-O3 | 167.9(3) |
| | | | Si-O3-Si | 137.1(2) |
| M1 octahedron | | | | |
| M1-O1A1,B1 | 2.157(4) | 2.157 | 2.176 | |
| M1-O1A2,B2 | 2.069(4) | 2.069 | 2.087 | |
| M1-O2C1,D1 | 2.081(4) | 2.082 | 2.105 | |
| Mean | 2.102 | 2.103 | 2.123 | |
| O1A1-O1B1 | 2.825(6) | 2.825 | 2.840 | 81.8(2) |
| O1A1-O1A2 (2x) | 3.072(3) | 3.072 | 3.084 | 93.2(1) |
| O1A1-O2C1 (2x) | 3.092(5) | 3.093 | 3.108 | 93.7(1) |
| O1A1-O1B2 (2x) | 2.840(6) | 2.840 | 2.855 | 84.4(1) |
| O1A2-O2C1 (2x) | 2.905(5) | 2.905 | 2.920 | 88.9(1) |
| O1A2-O2D1 (2x) | 3.017(5) | 3.017 | 3.032 | 93.3(2) |
| O2C1-O2D1 | 2.983(7) | 2.983 | 2.999 | 91.6(2) |
| Mean | 2.972 | 2.972 | 2.986 | |
| M2 polyhedron | | | | |
| M2-O1A1,B1 | 2.387(3) | 2.387 | 2.406 | |
| M2-O2C2,D2 | 2.352(4) | 2.353 | 2.375 | |
| M2-O3C1,D1 | 2.579(4) | 2.580 | 2.598 | |
| M2-O3C2,D2 | 2.779(4) | 2.779 | 2.795 | |
| Mean | 2.524 | 2.525 | 2.544 | |
| O1A1-O1B1 | 2.825(6) | 2.825 | 2.840 | 72.6(2) |
| O1A1-O2C2 (2x) | 3.185(5) | 3.186 | 3.200 | 84.5(1) |
| O1A1-O2D2 (2x) | 3.016(5) | 3.017 | 3.032 | 79.1(1) |
| O1A1-O3C1 (2x) | 4.282(5) | 4.282 | 4.291 | 119.1(1) |
| O1A1-O3C2 (2x) | 3.695(5) | 3.695 | 3.705 | 91.0(1) |
| O1A1-O3D1 (2x) | 4.617(5) | 4.617 | 4.625 | 136.8(1) |
| O1A1-O3D2 (2x) | 5.096(5) | 5.096 | 5.104 | 161.3(1) |
| O2C2-O2D2 | 4.630(8) | 4.630 | 4.640 | 159.5(2) |
| O2C2-O3C1 (2x) | 2.563(5) | 2.563 | 2.583 | 62.4(1) |
| O2C2-O3C2 (2x) | 4.183(5) | 4.183 | 4.193 | 108.9(1) |
| O2C2-O3D1 (2x) | 4.588(5) | 4.588 | 4.596 | 136.9(1) |
| O2C3-O3D2 (2x) | 3.434(5) | 3.434 | 3.446 | 83.6(1) |
| O3C1-O3C2 (2x) | 2.652(1) | 2.652 | 2.668 | 59.2(1) |
| O3C1-O3D1 | 3.389(6) | 3.389 | 3.401 | 82.2(2) |
| O3C1-O3D2 (2x) | 2.962(6) | 2.962 | 2.978 | 67.0(1) |
| O3C2-O3D2 | 4.452(7) | 4.452 | 4.462 | 106.5(2) |

*Corrections to interatomic distances after Busing and Levy (1964). See text for discussion of models.
†Atom notation based on Burnham et al. (1967).

their models are derived from application of inequalities that place bounds on the magnitude of the correction. The lower limit corresponds to highly correlated parallel motion and the upper limit describes highly correlated antiparallel motion. In a third model it is assumed that one atom "rides" on another. The thermal correction to the vector of separation is therefore dependent only on the motion of the first atom. The fourth model is valid for completely uncorrelated motion of the two atoms. Smyth (1973) argues that the correction to the distances in a pyroxene should lie between the noncorrelated model for weak interactions and the riding model for strong bonds. This conclusion should be amended since the riding model assumes a uni-directional interaction. If applicable to the strongest bonds of this structure, namely Si–O, the silicon atoms would have to be totally unaffected by the thermal motion of the oxygens; this is clearly not the case. Accordingly, the proper correction model for silicates should lie between the model for highly correlated parallel motion and that for non-correlated interactions. The uncorrected interatomic distances and angles and the corrected values using the two models described above are presented in Table 6.

When the bond distances obtained in this study are compared with the results of Clark *et al.* (1968, 1969) at room temperature and the results of CSPP at 700°C, the following observations may be made:

1. The tetrahedral chains are relatively unaffected by the heating. The mean Si–O distance is 1.635 Å at room temperature and 1.633 Å at 700°C, an insignificant change. This result agrees with previous high-temperature studies. The correction for thermal motion will tend to increase the interatomic distances; since these are very strong bonds, however, the effects will be minimal. The chain configuration is also affected very little by the heating. From room temperature to 700°C, the O3–O3–O3 angle changes only from 166.4° to 167.9° and the Si–O3–Si angle goes from 135.9° to 137.1°. These effects are much smaller than those from pigeonite (Brown, Prewitt, Papike, and Sueno, 1972).

2. The $M1$ octahedron and the $M2$ polyhedron expand significantly upon heating; however, this expansion is clearly not isotropic. In the $M1$ octahedron, the three crystallographically unique bonds increase by 0.004, 0.031, and 0.042 Å. The $M2$ polyhedron shows a similar anisotropy, the bond distances changing by −0.001, 0.018, 0.027, and 0.062 Å. The significance of the irregular bond expansion is discussed below. The two studies at 700°C agree well, the largest discrepancy being equal to 0.014 ± 0.005 Å. The mean values of the bond distances for the $M$-site cations differ by only one standard deviation.

## Thermal expansion of diopside

When a crystal undergoes thermal expansion, a spherical volume element at the original temperature will in general be deformed into an ellipsoid. The proper interpretation of this expansion may be given only if the principal values and axes of this ellipsoid are known. For crystals with orthorhombic and higher symmetries, the orientation of the ellipsoid is completely constrained and the principal values may be computed by inspection of the unit-cell parameters. However, for triclinic crystals there are no constraints, and for monoclinic crystals the direction of only one axis is required by the geometry. In such cases a calculation similar to that performed by the computer program STRAIN (Ohashi and Burnham, 1973: Ohashi and Finger, 1973) must be undertaken to ascertain the principal components of the expansion ellipsoid. A similar calculation for the monoclinic system has been described by Bouvast and Weigel (1970).

Program STRAIN has been used to calculate the ellipsoid components and associated errors for the diopside unit-cell data of this study, Deganello (1973), and CSPP. The results are presented in Table 7. An ellipsoid was computed for each temperature interval listed. Although the large standard deviations of these quantities make it impossible to resolve fine details of the expansion, the following general observations may be made:

1. Within the resolution of the available data, the linear and volume expansion coefficients are independent of temperature for the range studied. This result is in agreement with the temperature variation of the unit-cell volume, as shown in Figure 2. A least-squares computer program was used to determine the coefficients for polynomials to fourth order in the temperature using only the data from Table 2. Applying standard tests, the linear result shown in the diagram gave the most significant fit to the data.

2. The calculation of the standard axial expansion coefficients does not yield sufficient information to explain the dilation mechanisms and may lead to erroneous conclusions. For example, the $c$ axis exhibits the smallest coefficient of axial expansion, suggesting that the tetrahedral chains are constraining the expansion. In fact, the principal axis of minimum expansion is not in this direction but is rotated approximately 40° from $c$ toward $a$. The coefficient of

TABLE 7. Principal Thermal Expansion Coefficients for Diopside

| Temperature Range, °C | Reference* | Principal Linear Thermal Expansion Coefficients x $10^{-6}$ per degree | | | Volume Expansion Coefficients x $10^{-6}$ per degree | Orientations** | | |
|---|---|---|---|---|---|---|---|---|
| | | $\epsilon_1$ | $\epsilon_2$ | $\epsilon_3$ | | $\epsilon_1$ | $\epsilon_2$ | $\epsilon_3$ |
| 24-100 | 1 | 20.6(63) | 9.6(53) | -0.6(76) | 30(12) | b | 153(27) | 63(27) |
| 100-200 | 1 | 15.7(56) | 12.6(55) | 1.9(51) | 30(10) | b | 127(20) | 37(20) |
| 200-300 | 1 | 16.1(86) | 4.5(90) | -2.3(70) | 18(15) | 49(18) | b | -41(18) |
| 300-400 | 1 | 27.9(90) | 14.9(76) | 3.1(79) | 46(14) | b | 33(26) | 123(26) |
| 400-500 | 1 | 20.0(50) | 11.8(49) | 1.6(46) | 33(8) | b | 129(19) | 39(19) |
| 500-600 | 1 | 20.0(31) | 11.9(36) | 7.8(38) | 40(6) | b | 130(37) | 40(37) |
| 600-700 | 1 | 16.6(40) | 9.5(54) | 4.4(49) | 31(9) | b | 120(40) | 30(40) |
| 700-800 | 1 | 26.6(74) | 7.8(65) | 0.1(76) | 34(13) | b | 134(40) | 44(40) |
| 24-400 | 2 | 23.9(15) | 13.6(20) | -1.4(25) | 36(4) | b | 143(7) | 53(7) |
| 400-700 | 2 | 18.6(5) | 8.2(5) | 3.1(9) | 30(1) | b | 121(5) | 31(5) |
| 700-850 | 2 | 15.5(10) | 7.6(18) | 4.7(10) | 28(2) | b | 8(17) | 98(17) |
| 850-1000 | 2 | 22.8(10) | 11.6(30) | 6.3(39) | 41(5) | b | 84(22) | -6(22) |
| 25-325† | 3 | 17.2(5) | 9.2(8) | 4.3(13) | 31(1) | b | 138(6) | 48(6) |
| 325-625 | 3 | 17.8(15) | 10.6(13) | 2.7(18) | 31(2) | b | 142(6) | 52(6) |
| 625-825 | 3 | 21.1(23) | 11.5(14) | 6.5(24) | 39(4) | b | 8(17) | 98(17) |
| Weighted mean†† | | 18.5(22) | 8.9(14) | 3.7(20) | 31(3) | | | |

*References: (1) This study, (2) Cameron et al. (1973), (3) Deganello (1973).

**One of the principal axes is constrained to be parallel to $b$. The angles for the other principal axes are measured from $c$ toward $a$ in (010).

†The value of b at room temperature was taken as 8.924 Å (Deganello, pers. comm.).

††Weighted mean = $\Sigma_i(x_i/\sigma_{x_i}^2)\cdot\Sigma\sigma_{x_i}^2$.

expansion for this direction is roughly one-half the value parallel to $c$ and may be zero since its value is less than twice its standard deviation. Although the tetrahedral chains are undergoing very limited changes during the heating, they do not directly constrain the direction of minimal dilation. On the contrary, this direction corresponds very closely to the direction of the $M2$–O2$C2$, ($D2$) bonds as shown by Figure 3, a projection of the $M2$ polyhedron parallel to $b$. These are the bond lengths that apparently shrink as the crystal is heated from room temperature to 700°C. This agrees with the results of Ohashi and Burnham (1973) who found that the shortest $M2$–O bond distance corresponds closely to the minimum expansion direction for thermal changes; however, this direction undergoes the greatest change if the size of the $M2$ cation is changed.

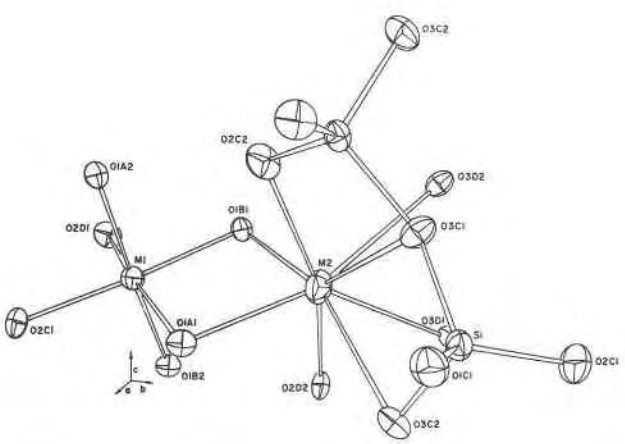


FIG. 1. A coordination diagram for diopside at 700°C projected approximately parallel to [16,6,11]. The thermal ellipsoids are scaled to represent 50 percent probability. The atom nomenclature is from Burnham *et al.* (1967), and the computer program ORTEP-II (Johnson, 1965, 1970) was used in the preparation of the diagram.

3. The direction of the maximum thermal expansion is parallel to $b$. An examination of the distortions of the polyhedra about the $M$ sites will be required to explain this result since the edge-sharing prevents expansion from $M$-site polyhedral tilting (Megaw, 1971). One explanation is that dilation in this direction does not require any expansion of the tetrahedral chain. If the bond distances and angles of Table 6 are compared with similar quantities for the results at room temperature, it may be seen that the O–$M2$–O angles increase when both oxygens

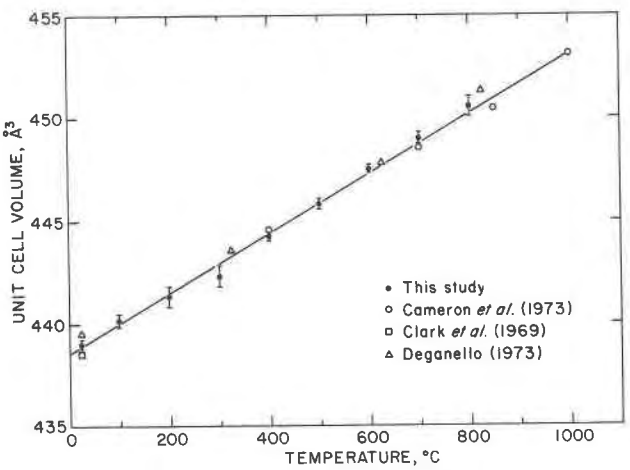


FIG. 2. Variation of unit-cell volume with temperature for diopside. The error bars represent ±1 standard deviation. A least-squares technique with the data from this study only was used to calculate the coefficients of the line. The results of Nolan and Edgar (1963) at room temperature would plot at the same position as those of Deganello (1973).

are shared with the *M*1 octahedral strip and decrease when the oxygens are shared with the tetrahedral chain. For example the O1*A*1–*M*2–O1*B*1 angle increases by 0.4° whereas the O3*C*1–*M*2–O3*C*2 angle decreases by 3.7°. Because the O3*C*1–O3*C*2 distance is essentially unchanged (0.008 Å), this relatively large change in the angle must be attributed to a motion of these oxygens away from *M*2. As noted earlier, the tetrahedral chain lengths and angles are essentially unchanged during the expansion, causing them to be displaced parallel to *b* as a unit. This displacement forces a change in the O2 position, which results in a 2.0° change in the O2*C*2–*M*2–O2*D*2 angle. There are concomitant changes in the *M*1 octahedron. The bond angles that show the greatest changes are those involving O2. For example, the O2*C*1–*M*1–O1*A*1 angle increases by 1.0°, whereas the O2*C*1–*M*1–O2*D*1 angle decreases by 1.7°. This latter change is again the result of the motion of O2 essentially parallel to *b* (the O2*C*1–O2*D*1 distance is unaffected). The major effects of the expansion seem to be a lengthening of the *M*2–O3 bonds with a translation of the tetrahedral chains. In turn, this forces a readjustment of the *M*1–O2 configuration. It is interesting to note that these changes in the *M*1 octahedron do not cause a major change in the distortion of the polyhedron. The quadratic elongation changes only from 1.0052 at room temperature to 1.0058 at 700°C, and the range of the bond angle variance is 17.4 to 18.5. These parameters have been proposed by Robinson, Gibbs, and Ribbe (1971) as sensitive to the distortion. The *M*2 polyhedron becomes more distorted with increasing temperature because the *M*2–O3 bonds, which are the longest, increase more than the others.

Although there are significant changes between the structure of diopside at room temperature and that at 700°C, there is no evidence of any major structural changes that would lead to the melting of the structure. When the observed changes are extrapolated to the melting point (1391.5°C), the resulting bond distances are normal. It is reasonable to assume that the mechanism of expansion may change as the melting point is approached.

## Conclusions

The principal conclusions of this study are:

1. The details of the expansion for monoclinic or triclinic material may be misinterpreted unless the principal strain components are calculated.

2. The direction of minimum expansion is more

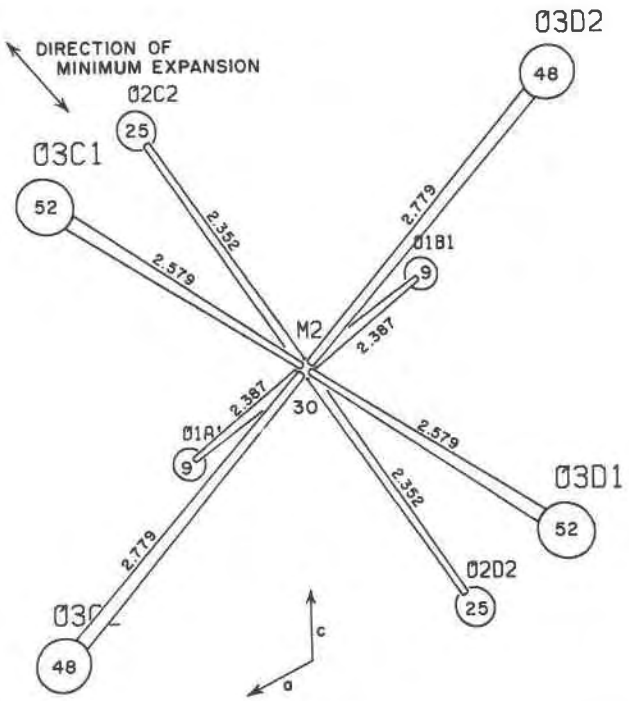


FIG. 3. A coordination diagram for the *M*2 polyhedron of diopside at 700°C with the bond distances shown. The projection is parallel to *b*. The computer program ORTEP-II was used in the preparation of this diagram. The sizes of the circles marking the atom positions do not represent thermal vibration but are intended to indicate the vertical position which is given as a percentage of the *b* axis by the numbers associated with the atom. The correlation between the directions of the shortest *M*2–O bonds and the minimum expansion is also indicated.

highly correlated with the shortest $M2$–O distance than with the direction of the chain of silica tetrahedra in spite of the relatively small changes undergone by this chain.

3. The results of the two studies of the crystal structure of diopside at high temperature are essentially identical even though very different techniques were used to perform the analyses. If small differences are observed in the results of future comparative high-temperature studies, more confidence may be placed in the interpretation that these represent real differences in the structures.

## Acknowledgments

The authors gratefully acknowledge the contributions of L. C. Garver and C. G. Hadidiacos, whose workmanship facilitated the construction of the crystal heater and temperature controller. Valuable suggestions for changes in the manuscript were given by J. J. Papike and C. T. Prewitt of the State University of New York at Stony Brook, Charles W. Burnham of Harvard University, and D. Virgo and R. H. McCallister of the Geophysical Laboratory.

## References

Bouvast, J. and D. Weigel (1970) Sesquioxide de plomb, $Pb_2O_3$. II. Etude de la dilutation thermique d'un monocrystal. *Acta Crystallogr.* **A26,** 510–514.

Brown, G. E., C. T. Prewitt, J. J. Papike and S. Sueno (1972) A comparison of the structures of high and low pigeonite. *J. Geophys. Res.* **77,** 5778–5789.

Burnham, Charles W. (1966) Computation of absorption corrections and the significance of end effect. *Am. Mineral.* **51,** 159–167.

———, Joan R. Clark, J. J. Papike and C. T. Prewitt (1967) A proposed crystallographic nomenclature for clinopyroxene structure. *Z. Kristallogr.* **125,** 109–119.

Busing, William R. (1970) Least-squares refinement of lattice and orientation parameters for use in automatic diffractometry. In, F. R. Ahmed, Ed., *Crystallographic Computing,* Munksgaard, Copenhagen, p. 319–330.

——— and Henry A. Levy (1964) The effect of thermal motion on the estimation of bond lengths from diffraction measurements. *Acta Crystallogr.* **17,** 142–146.

Cameron, Maryellen, Shigeho Sueno, C. T. Prewitt and J. J. Papike (1973) High-temperature crystal chemistry of acmite, diopside, hedenbergite, jadeite, spodumene, and ureyite. *Am. Mineral.* **58,** 594–618.

Chesterman, C. W. (1942) Contact metamorphic rocks of the Twin Lakes region, Fresno County, California. *Calif. J. Mines Geol.* **38,** 243–281.

Clark, Joan R., Daniel E. Appleman and J. J. Papike (1968) Bonding in eight ordered clinopyroxenes isostructural with diopside. *Contrib. Mineral. Petrol.* **20,** 81–85.

———, ——— and ——— (1969) Crystal-chemical characterization of clinopyroxenes based on eight new structure refinements. *Mineral. Soc. Am. Spec. Pap.* **2,** 31–50.

Cromer, Don T. and David Liberman (1970) Relativistic calculation of anomalous scattering factors for X rays. *J. Chem. Phys.* **53,** 1891–1898.

——— and Joseph B. Mann (1968) X-ray scattering factors computed from numerical Hartree-Fock wave functions. *Acta Crystallogr.* **A34,** 321–324.

Deganello, Sergio (1973) The thermal expansion of a diopside. *Z. Kristallogr.* **137,** 127–131.

Finger, L. W. (1973) A low-cost automated diffractometer system employing a high-level programming language (abstr.). *Am. Crystallogr. Assoc.,* Storrs Meeting, p. 140.

———, C. G. Hadidiacos and Y. Ohashi (1973) A computer-automated, single-crystal X-ray diffractometer. *Carnegie Inst. Wash. Year Book,* **72,** 694–699.

——— and E. Prince (1975) A system of Fortran IV computer programs for crystal structure computations. *Natl. Bur. Stand. Tech. Note,* **854,** 128 p.

Gabe, E. J., G. E. Alexander and R. H. Goodman (1970) The Mines Branch on-line single-crystal diffractometer. *Mineral. Sci. Div., Can. Dep. Energy, Mines, Resour., Internal Rep.* MS **71-54.**

Hamilton, W. C. (1959) On the isotropic temperature factor equivalent to a given anisotropic temperature factor. *Acta Crystallogr.* **12,** 609–610.

Johnson, Carroll K. (1965) Ortep: A Fortran thermal-ellipsoid plot program for crystal structure illustrations. *ORNL-3794 Revised,* Oak Ridge National Laboratory, Oak Ridge, Tennessee.

——— (1970) Drawing crystal structures by computer. In, F. R. Ahmed, Ed., *Crystallographic Computing,* Munksgaard, Copenhagen, p. 227–230.

Korn, Granino A. and Theresa M. Korn (1961) *Mathematical Handbook for Scientists and Engineers.* McGraw-Hill, New York.

Megaw, Helen D. (1971) Crystal structures and thermal expansion. *Mater. Res. Bull.* **6,** 1007–1018.

Nolan, J. and A. D. Edgar (1963) An X-ray investigation of synthetic pyroxenes in the system acmite-diopside-water at 1000 kg/cm² water vapour pressure. *Mineral. Mag.* **33,** 625–634.

Ohashi, Yoshikazu and Charles W. Burnham (1973) Clinopyroxene lattice deformations: The roles of chemical substitution and temperature. *Am. Mineral.* **58,** 843–849.

——— and L. W. Finger (1973) Lattice deformations in feldspars. *Carnegie Inst. Wash. Year Book,* **72,** 569–573.

Robinson, K., G. V. Gibbs and P. H. Ribbe (1971) Quadratic elongations: A quantitative measure of distortion in coordination polyhedra. *Science,* **172,** 567–570.

Smyth, Joseph R. (1973) An orthopyroxene structure. *Am. Mineral.* **58,** 636–648.

Tichý, K. (1970) A least-squares method for the determination of the orientation matrix in single-crystal diffractometry. *Acta Crystallogr.* **A26,** 295–296.

Warren, B. and W. L. Bragg (1928) The structure of diopside $CaMg(SiO_3)_2$. *Z. Kristallogr.* **69,** 168–193.

Zachariasen, W. H. (1968) Experimental tests of the general formula for the integrated intensity of a real crystal. *Acta Crystallogr.* **A24,** 212–216.

*Manuscript received, June 5, 1975; accepted for publication, July 31, 1975.*